ELSEVIER

Spin-up of a double-diffusive fluid in a cylinder

Chang Ho Lee and Jae Min Hyun
Department of Mechanical Engineering, Korea Advanced Institute of Science and Technology, Yusungku, Taejon, South Korea

A numerical study is made of the linearized spin-up process of a double-diffusive fluid in a vertically mounted cylindrical vessel of aspect ratio $O(1)$. Both the temperature and concentration conditions render gravitationally stable contributions to the overall density profile. Numerical solutions are acquired to the time-dependent axisymmetric Navier–Stokes equations, using the standard Boussinesq fluid approximations. The major nondimensional parameters are identified. Results are compiled for small Ekman number, the Prandtl number $\sim O(1)$, and broad ranges of the stratification number St, buoyancy ratio R_ρ, and Lewis number Le, are dealt with. The evolution of the azimuthal velocities is described, and the attendant meridional flows are depicted. The global spin-up process is retarded for a double-diffusive fluid, and this trend is more pronounced as R_ρ increases. The spatial nonuniformity of the rate of spin-up is enhanced as St and R_ρ increase. The effects of double-diffusion on the fields of perturbation density, temperature, and concentration are plotted. The impact of Le on spin-up is illustrated, and the plots of the perturbation physical variables of interest are presented.

Keywords: spin-up; double-diffusive fluid; stratified flow

Introduction

Spin-up refers to the transient adjustment process of a fluid from one state of rigid-body rotation to another of different rotation rate. This classical flow model has been center stage in the research of transient rotating fluid dynamics and associated transport phenomena. Applications can be found in a diverse array of geophysical fluid systems, as well as in rotating machinery.

For definiteness, the model-building efforts have been directed to the case of an incompressible fluid, which completely fills a vertically mounted, closed cylindrical container of aspect ratio $O(1)$. A major nondimensional parameter is the Ekman number $E \equiv \nu/\Omega_i H^2$, in which ν denotes the kinematic viscosity of the fluid, Ω_i the rotation rate of the initial state, and H the characteristic dimension of the container. For most relevant applications, $E \ll 1$. This implies that the principal effects of viscosity are confined to thin boundary layers on the solid boundary walls. When the change in the rotation rate of the container between the initial state (Ω_i) and the final state ($\Omega_i + \Delta\Omega$) is small; i.e., the Rossby number $\varepsilon \equiv \Delta\Omega/\Omega_i \ll 1$, Greenspan and Howard (1963) presented a linearized analysis for a homogeneous fluid. It was clearly demonstrated that the Ekman boundary layers form on the endwall disks, which, in turn, generate meridional circulation. In the interior, the radially inward meridional motions bring forth an increase of angular velocity by virtue of angular momentum conservation. It is significant to note that the adjustment process in the bulk of interior is substantially accomplished over the so-called spin-up time-scale $\tau_s \sim O(E^{-\frac{1}{2}}\Omega_i^{-1})$, rather than the usual diffusive time-scale $\tau_d \sim O(E^{-1}\Omega_i^{-1})$. The fundamental notions of this model have since been verified by numerical and experimental endeavors (e.g., Warn-Varnas et al. 1978).

Studies on spin-up of a stably stratified fluid disclosed that the Ekman layer-induced meridional circulation is still the most prominent dynamical element (Walin 1969; Sakurai 1969). However, because of suppression of the vertical motions by stratification, the meridional flows do not fill the entire interior of the container. Consequently, the spin-up process in the interior proceeds in a spatially nonuniform manner. The fluids in the areas near the endwall disks approach the final-state rotation faster than in the areas near the midheight of the cylinder. In the investigations above, the variation of the fluid density is caused by either a temperature or a concentration difference that is imposed between the two horizontal endwall disks of the cylinder (Buzyna and Veronis 1971; Saunders and Beardsley 1975). Detailed descriptions of the flow and temperature fields were given in the numerical solutions by Hyun et al. (1982).

As pointed out earlier, the preceding studies on spin-up dealt with the situations in which the variation of the fluid density stems from the nonuniformity of a single diffusing agent; i.e., temperature(heat) or concentration. The simultaneous presence of two (or possibly more) diffusing agents; e.g., temperature and concentration, generally has been known to lead to complex flow patterns and transport properties in the fluid system (e.g., see the review article of Turner 1974). Numerous accounts have been given in the literature to depict these double-diffusive convective

Address reprint requests to Dr. J. M. Hyun, Korea Advanced Institute of Science and Technology, Yusungku, Taejon, 305-701, South Korea.

Received 23 April 1996; accepted 31 January 1997

Int. J. Heat and Fluid Flow 18: 507–517, 1997

655 Avenue of the Americas, New York, NY 10010

0142-727X/97/$17.00
PII S0142-727X(97)00030-1

flows in a nonrotating framework under pertinent boundary conditions (e.g. Lee and Hyun 1991a, b; Hyun and Lee 1990; Ostrach et al. 1987). The importance of this subject matter in a rotating environment is recognized in recent industrial applications, such as the Czochralski technique in growing single crystals (Kobayashi 1980; Brown 1988; Sung et al. 1993, 1995). In this case, the melt is in a rotating container, and the density of the melt is determined by the combined fields of temperature and concentration. The findings of the present study may not be of direct quantitative relevance to actual crystal growth applications, because the pertinent parameters are not precisely matched to those in the applications. However, the overall qualitative trends can be captured by the present endeavors.

In the context of spin-up, the transient flow and transport characteristics of a double-diffusive fluid warrant in-depth examination. In the present work, numerical solutions are acquired for the fundamental flow model of the linearized spin-up for small Ekman number. The principal nondimensional parameters are identified, and the time-dependent velocity, temperature and concentration fields are described for varying dimensionless parameters. A key ingredient of the solution is to demonstrate the degrees of advancement of spin-up for large Lewis numbers, which are typical of realistic crystal growth situations.

Recall that the principal focus of the present study is directed to linearized flow regimes in which $\varepsilon \ll 1$. In many applications, however, a significant problem is the spin-up process from the initial state of rest, which is characterized by strong nonlinearities. An elegant nonlinear flow model for a homogeneous fluid was brought forth by Wedemeyer (1964), and it was subsequently refined for a single-diffusive stratified fluid (Greenspan 1980; Hyun 1983). A study of the spin-up from rest of a double-diffusive stratified fluid is underway, and the results are to be reported in a later account.

Formulation

Consider a vertically mounted right circular cylindrical container (height H, radius R), completely filled with an incompressible fluid. The cylindrical coordinates (r, θ, z) are defined as shown in Figure 1.

At the initial state, the fluid and the container are in rigid-body rotation with angular velocity Ω_i. The temperature and concentration are, respectively, T_H and S_L at the top horizontal endwall disk ($z = H/2$), and T_L and S_H at the bottom horizontal endwall disk ($z = -H/2$). Note that, in the present problem setup, both temperature and concentration make stabilizing contributions to the overall density stratification; i.e., $\Delta T\ (\equiv T_H - T_L) > 0$ and $\Delta S\ (\equiv S_H - S_L) > 0$. The cylindrical sidewall ($r = R$) is thermally insulated and impervious to concentration flux. Furthermore, it is assumed that $\Omega_i^2 H/g \ll 1$ so that the Sweet–Eddington flow can be neglected (Buzyna and Veronis 1971), and at the initial state, no relative internal flow is allowed. At the initial instant $t = 0$, the rotation rate of the container is abruptly increased to

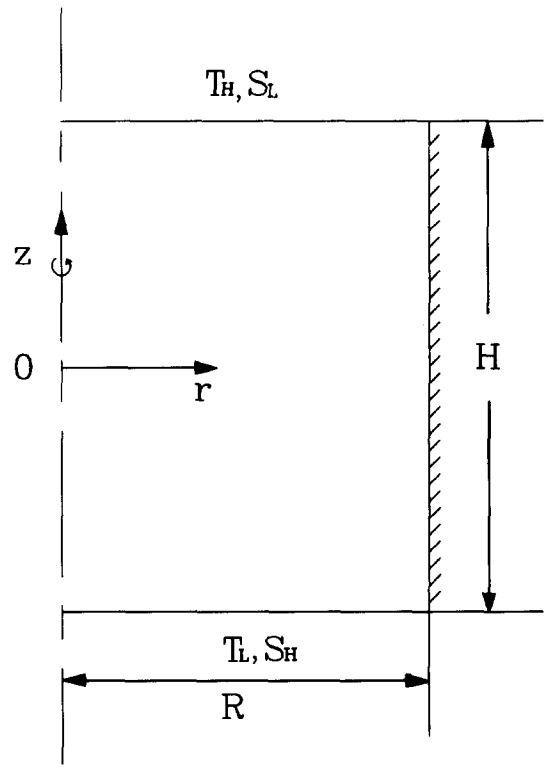

Figure 1 Flow configuration and coordinate system

Notation

Ar	aspect ratio
E	Ekman number
H	height of cylinder
Le	Lewis number
N	Brunt–Väisälä frequency
p	dimensionless reduced pressure
Pr	Prandtl number
R	radius of cylinder
R_ρ	buoyancy ratio
St	overall stratification parameter
S	dimensionless concentration
S_i	initial concentration
S'	perturbation concentration
T	dimensionless temperature
T_i	initial temperature
T'	perturbation temperature
u	dimensionless radial velocity
v	dimensionless azimuthal velocity
w	dimensionless vertical velocity
r, θ, z	cylindrical coordinates

Greek

α_T	thermal expansion coefficient
α_S	solutal expansion coefficient
β_S	solutal Rossby number
β_T	thermal Rossby number
ΔT	temperature difference between top and bottom endwall disks
ΔS	concentration difference between top and bottom endwall disks
$\Delta\Omega$	angular velocity difference
κ_T	thermal diffusivity
κ_S	solutal diffusivity
ν	kinematic viscosity
ρ	dimensionless density
ρ_o	reference density
ρ_i	initial density
ρ'	perturbation density
τ	dimensionless spin-up time scale ($= E^{-\frac{1}{2}}$)
Ω_f	final angular velocity
Ω_i	initial angular velocity

$\Omega_i + \Delta\Omega$, and the resulting time-dependent flow of the interior fluid is to be examined. As an extension of the prior works, the Rossby number $\varepsilon[\equiv \Delta\Omega/\Omega_i] \ll 1$, which permits a linearized analysis of the problem.

The Boussinesq approximation is invoked to express the variation of density ρ:

$$\rho = \rho_o[1 - \alpha_T(T - T_o) + \alpha_S(S - S_o)] \tag{1}$$

In the above, subscript o denotes the reference values, and α_T and α_S refer, respectively, to the coefficients of volumetric expansion with respect to temperature T and concentration S. In accordance with the Boussinesq fluid assumption, all the physical properties are taken to be constant. It is advantageous to introduce the nondimensionalized quantities (asterisks), which are related to their dimensional counterparts (no asterisks) in the following fashion:

$$t^* = t\Omega_i;\ (u^*, v^*, w^*) = (u, v, w)/R\Omega_i;\ (r^*, z^*) = (r, z)/H;$$

$$S^* = \frac{S - S_o}{\Delta S};\ T^* = \frac{T - T_o}{\Delta T}$$

The governing, properly nondimensionalized, time-dependent, full, axisymmetric Navier–Stokes equations, written in a cylindrical frame rotating at Ω_i with the corresponding velocity components (u^*, v^*, w^*), are (after dropping the asterisk):

$$\frac{1}{r}\frac{\partial}{\partial r}(ru) + \frac{\partial w}{\partial z} = 0 \tag{2}$$

$$\frac{\partial u}{\partial t} + u\frac{\partial u}{\partial r} + w\frac{\partial u}{\partial z} - \left(2 + \frac{v}{r}\right) r = -\frac{\partial p}{\partial r} + \mathrm{E}\left(\nabla^2 u - \frac{u}{r^2}\right) \tag{3}$$

$$\frac{\partial v}{\partial t} + u\frac{\partial v}{\partial r} + w\frac{\partial v}{\partial z} + \left(2 + \frac{v}{r}\right) u = \mathrm{E}\left(\nabla^2 v - \frac{v}{r^2}\right) \tag{4}$$

$$\frac{\partial w}{\partial t} + u\frac{\partial w}{\partial r} + w\frac{\partial w}{\partial z} = -\frac{\partial p}{\partial z} + \beta_T T - \beta_S S + \mathrm{E}\nabla^2 w \tag{5}$$

$$\frac{\partial T}{\partial t} + u\frac{\partial T}{\partial r} + w\frac{\partial T}{\partial z} = \frac{\mathrm{E}}{\mathrm{Pr}}\nabla^2 T \tag{6}$$

$$\frac{\partial S}{\partial t} + u\frac{\partial S}{\partial r} + w\frac{\partial S}{\partial z} = \frac{\mathrm{E}}{\mathrm{Pr\,Le}}\nabla^2 S \tag{7}$$

As stated earlier, in the initial state, the fluid is motionless with vertically linear distributions of temperature and concentration:

$$\frac{\partial T}{\partial z} = 1,\ \frac{\partial S}{\partial z} = -1,\ u = v = w = 0 \qquad \text{at} \qquad t = 0 \tag{8}$$

The boundary conditions, which reflect the instantaneous increase of the rotation rate of the container, are expressed as

$$T = 0,\ S = 0,\ \frac{\partial u}{\partial z} = \frac{\partial v}{\partial z} = w = 0 \qquad \text{at} \qquad z = 0 \tag{9a}$$

$$T = 0,\ S = 0,\ u = w = 0,\ v = r\varepsilon \qquad \text{at} \qquad z = -0.5 \tag{9b}$$

$$\frac{\partial T}{\partial r} = \frac{\partial S}{\partial r} = 0,\ u = w = 0,\ v = \left(\frac{R}{H}\right)\varepsilon \quad \text{at} \quad r = R/H \tag{9c}$$

$$\frac{\partial T}{\partial r} = \frac{\partial S}{\partial r} = 0,\ u = \frac{\partial (v/r)}{\partial r} = \frac{\partial w}{\partial r} = 0 \quad \text{at} \quad r = r_i \tag{9d}$$

Note that the problem formulation is antisymmetric with respect to the cylinder midheight $z = 0$. Therefore, only the bottom half of the cylinder is considered (Equations 9a–c). Also, in order to meet the numerical stability requirements at the central axis $r = 0$, the axis conditions are applied at a small, but finite, value $r = r_i$. This kind of treatment of the axis conditions, which perhaps is not a completely settled issue, has been widely used in practice and discussed at length (Warn-Varnas et al. 1978; Hyun et al. 1982; Hyun and Kwak 1989; Lang et al. 1994). In the present work, in several exemplary calculations, the computed results at a typical interior point; e.g., the midradius and quarter-height point, differed less than 0.1% as r_i changed from 0.001 to 0.01. In most runs, r_i was set 0.005.

The pertinent dimensionless parameters that emerge in the equations are

Ekman number:

$$E = \frac{\nu}{\Omega_i H^2}$$

Rossby number:

$$\varepsilon = \frac{\Delta\Omega}{\Omega_i}$$

Prandtl number:

$$\mathrm{Pr} = \frac{\nu}{\kappa_T}$$

Lewis number:

$$\mathrm{Le} = \frac{\kappa_T}{\kappa_S}$$

Buoyancy number:

$$R_\rho = \frac{\alpha_S \Delta S}{\alpha_T \Delta T}$$

Stratification number:

$$\mathrm{St} = \left(\frac{N}{\Omega_i}\right)^2$$

where the Brunt–Väisälä frequency is defined

$$N = [(\alpha_T g\Delta T + \alpha_S g\Delta S)/H]^{\frac{1}{2}}$$

Thermal Rossby number:

$$\beta_T = \alpha_T g\Delta T/H\Omega_i^2$$

Solutal Rossby number:

$$\beta_S = \alpha_S g\Delta S/H\Omega_i^2$$

In the above, κ_T and κ_S refer, respectively, to the thermal and concentration diffusivities. The Lewis number Le indicates their

ratio, and in many double-diffusive situations of practical interest, Le is much larger than unity. This implies that heat is diffused at a much higher rate than concentration. The buoyancy ratio R_ρ denotes the contribution of solutal stratification, relative to that of thermal stratification, in the make-up of the total density stratification. The effect of overall fluid stratification, in comparison to the effect of rotation, is measured by St.

In passing, if the T and S variations make opposing contributions to the overall density stratification, the global flow pattern is anticipated to be strongly characterized by the value of Le. This flow configuration will be examined in the forthcoming research endeavors.

Numerical solutions to the above system of equations were obtained by adopting the well-established SIMPLER algorithm (Patankar 1980). The specifics of this numerical procedure have been documented extensively, and computations were straightforward. Staggered and stretched mesh networks were deployed, and the grid points used were typically (40×40) in the $(r \times z)$ axial plane. The time interval Δt was $3.85 \times 10^{-4} \tau_S$. The grid-stretching was implemented so that typically eight grid points are placed within the Ekman boundary layer. Grid-convergence tests were conducted by repeating calculations for several sample runs by using grids (40×40) and (80×80). The corresponding changes in the results at the cylinder midradius, quarter-height were less than 0.1%. Also, time-step-convergence tests were performed by deploying Δt at $3.85 \times 10^{-4}\tau$, and $3.85 \times 10^{-5}\tau$. Again, the variations in the results were smaller than 0.1%. Furthermore, some of the well-known higher-order differencing schemes (Hayase et al. 1992; Patankar 1980) were employed, and the results of these exercises were highly mutually consistent for the parameter values of present concern.

Results and Discussion

Time-marching solutions were secured for broad ranges of principal nondimensional parameters. In view of the presence of a large number of parameters, attention was focused to the qualitative changes in flow characteristics as St, R_ρ, Le, and E are altered. To facilitate direct comparisons with the previous accounts on single-diffusive spin-up, it was set Ar = 1.0, Pr = 1.0, and $\varepsilon = 0.05$ to simulate linearized problems.

First, Figures 2 and 3 display the progress of spin-up, as exhibited by the evolution of the azimuthal velocity, $(v/r\varepsilon)$, at different radial and axial locations. The Ekman number was set $E = 1.41 \times 10^{-3}$, and, to simulate realistic double-diffusive convection problems, Le = 100. Time is normalized by using the spin-up time-scale $\tau \equiv E^{-\frac{1}{2}}$, which was ascertained in the classical analysis by Greenspan and Howard (1963). Plot (a) illustrates the case of nonstratified(homogeneous) fluid spin-up; i.e., St = 0. Plots (b), (c), and (d) exemplify the results of a stratified fluid by setting St = 10.0, but with different values of the buoyancy ratio R_ρ. The case of $R_\rho = 0$, shown in plot (b), corresponds to the spin-up of a single-diffusive fluid; i.e., the only diffusing agent is temperature. As seen in Figure 2 for $z = 0$, the region in the vicinity of the sidewall is heavily influenced by viscous effects. Spin-up in this area proceeds at a fast rate. In the interior region; i.e., at small and moderate radii, the dominant mechanism for spin-up for a homogeneous fluid is inviscid in nature. As expounded by Greenspan and Howard, the Ekman layer suctions at both endwall disks produce radially inward meridional motions in the interior. Angular momentum is conserved in the inviscid interior; therefore, the angular velocity at a given location increases with time as the radius of the fluid element decreases. As seen in plot (a) of Figure 2, the rate of increase of the scaled angular velocity $v/r\varepsilon$ is fairly uniform in the bulk of the interior. In the region close to the sidewall, the fluid adjustment process is heavily influenced by viscous effects, which yields a relatively rapid and smooth evolution. This feature is reproduced well in the present numerical computations.

For a stratified fluid, a different picture emerges. The rate of spin-up is not spatially uniform in the interior. In general, at midheight, spin-up proceeds at a slower rate for a stratified fluid than for a homogeneous fluid. This feature is explained by noting that, for a stratified fluid, the meridional circulation tends to be restricted in the regions close to the endwall disks. In other words, because of the inhibition of vertical velocities by stable stratification, the meridional flows cannot penetrate up to the midheight of the cylinder. Consequently, as seen in Figure 3, spin-up is enhanced(retarded) in the region close to the endwall (midheight) of the cylinder. This flow character was pointed out by Sakurai (1969) and Hyun et al. (1982, 1983) for the spin-up of a single-diffusive stratified fluid. The calculated data in Figures 2 and 3 support these earlier findings. Furthermore, under the same overall stratification, the rate of spin-up decreases as the buoyancy ratio R_ρ increases.

It is interesting to note the presence of high-frequency oscillations in the interior. For a homogeneous fluid, these oscillations are identified to be the inertial mode of frequency $2\Omega_i$ (Warn-Varnas et al. 1978). For a stratified fluid, the oscillations reflect the existence of modified inertial-internal gravity modes with higher frequencies than that of the inertial mode (Hyun et al. 1982). As asserted earlier, the relative effects of viscosity increase for a stratified fluid; therefore, these high-frequency oscillations are damped out faster as the strength of stratification increases.

Figure 3 illustrates the above-mentioned axial variations of $v/r\varepsilon$. Obviously, very close to the endwall, a viscously controlled Ekman layer is seen. For a homogeneous fluid, the rate of spin-up is substantially uniform in the interior (see plot a). However, axial variations of $v/r\varepsilon$ are appreciable for a stratified fluid, and this trend is more pronounced for a double-diffusive fluid with large R_ρ. The retardation of spin-up near the midheight is discernible in these plots.

The computational results are rearranged to display the systematic influences of the relevant parameters. Figure 4 exhibits the explicit effect of St on the spin-up at the midheight, midradius of the cylinder $[z = 0,\ r = 0.5]$. The slowing-down of spin-up with increasing stratification is in evidence. The impact of R_ρ is shown in Figure 5, which underscores the retardation of spin-up as R_ρ increases. These features are in line with the physical explanations which were put forth earlier.

The patterns of the meridional flows of a double-diffusive fluid are illustrated in Figure 6. The meridional stream function Ψ (dimensional) is defined so that $u^* = (1/r^*)(\partial\Psi^*/\partial z^*)$, $w^* = -(1/r^*)(\partial\Psi^*/\partial r^*)$. The present problem formulation is antisymmetric with respect to the cylinder midheight $(z = 0)$; therefore, only the bottom half of the cylinder is shown. For a nonstratified fluid (see Figure 6a for St = 0), the counterclockwise meridional circulation fills the entire cavity, as stressed earlier (Warn-Varnas et al. 1978). As illustrated in Figure 6b, the fluid stratification suppresses vertical motions; therefore, the extent of meridional circulation is restricted closer to the endwall disks. This trend becomes more pronounced as the fluid is double-diffusively stratified. As shown in Figures 6c and d, the meridional flow weakens in strength and shrinks in size. It is important to observe that for the same value of St, as R_ρ increases, the meridional flows weaken, and the extent of the counterclockwise cell is confined to a region close to the endwall. In summary, the depiction of the meridional flows indicates that an increase of R_ρ, under the same overall stratification, is equivalent to an increase of St for a single-diffusive fluid.

To delineate the specific impacts of the parameters of a double-diffusive fluid, the fields of perturbation quantities in the axial plane are depicted. For this purpose, the perturbation

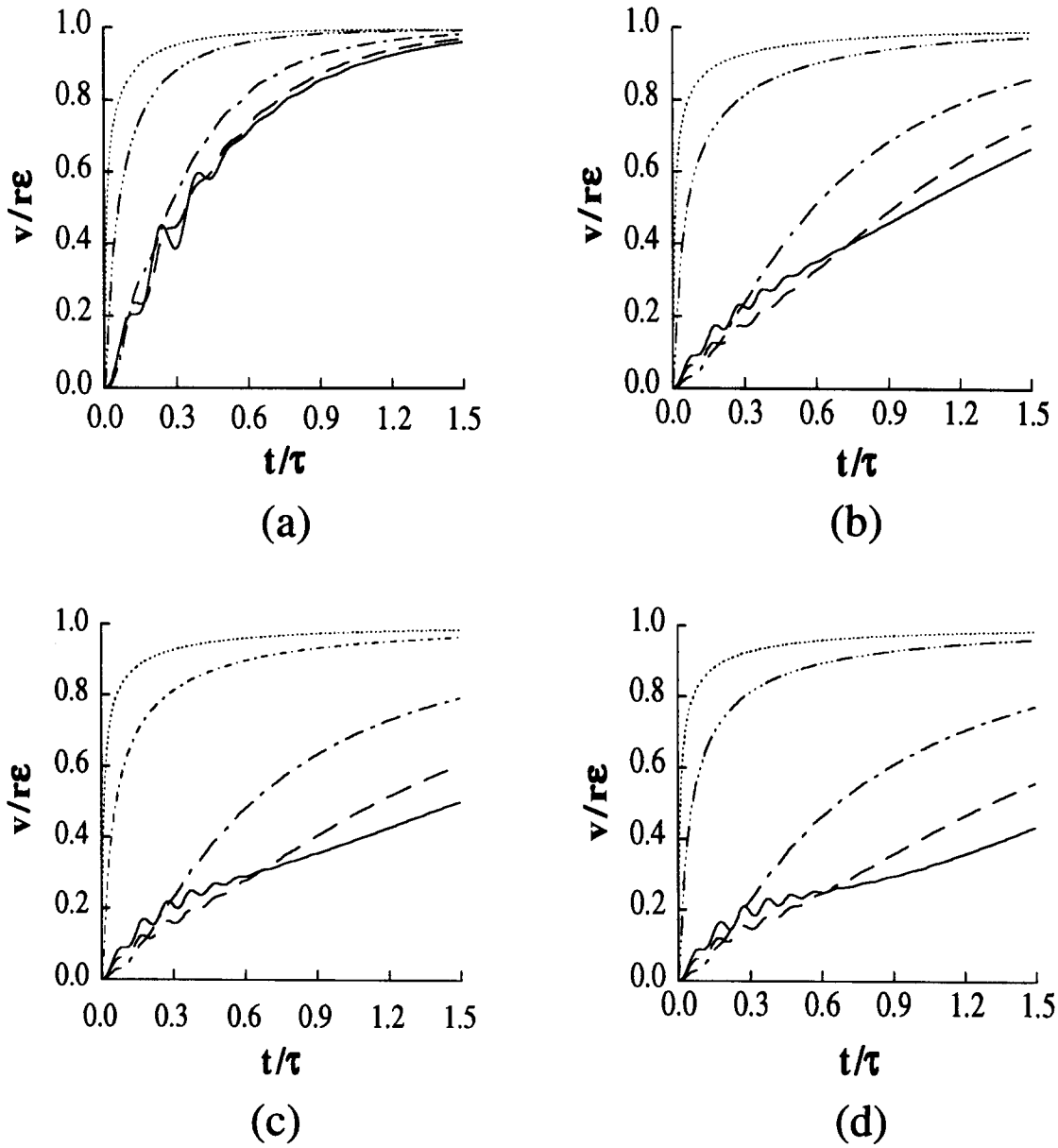

Figure 2 Evolution of normalized azimuthal velocity, $v/r\varepsilon$, at midheight $z=0$, $E=1.41\times10^{-3}$; conditions: (a) homogeneous fluid (St=0); (b) single-diffusive fluid (St=10.0, $R_\rho=0$); (c) double-diffusive fluid (St=10.0, $R_\rho=1.0$); (d) double-diffusive fluid (St=10.0, $R_\rho=10.0$); radial positions r: $r=0.25$,——; 0.51, – –; 0.75, —·—; 0.95, —···—; 0.98, ·····

density ρ' is defined as (Saunders and Beardsley 1975):

$$\rho' = \frac{g}{\Omega_i^2 H\varepsilon}[\rho - \rho_i(z)]$$

in which ρ and $\rho_i(z)$ denote the instantaneous density and the initial-state density, respectively. Similarly, the perturbation temperature T' and the perturbation concentration S' are introduced

$$T' = \frac{\beta_T}{\varepsilon}[T - T_i(z)]$$

$$S' = \frac{\beta_S}{\varepsilon}[S - S_i(z)]$$

Figure 7 is an exemplary plot of ρ' in the bottom half of the cylinder. In general, as a result of spin-up flows, the density at small and moderate radii is smaller than the initial value; i.e., $\rho' < 0$; and at large radii, $\rho' > 0$. This can be explained by noting the existence of a counterclockwise meridional cell, as shown in Figure 6. At large radii, the counterclockwise motion brings the fluid of high density from below, which, therefore, causes positive perturbation densities. At small and moderate radii, the axial flows are toward the endwall, which carry the fluid of low density from above; negative perturbation densities are observed in these regions. The magnitudes of perturbation densities tend to be augmented in the vicinity of the endwall, as R_ρ increases. This is expected in view of the clustering of meridional flows in the neighborhood of the endwall, as R_ρ increases.

The perturbation temperatures are plotted in Figure 8. Because of the action of meridional flows, fluids of low tempera-

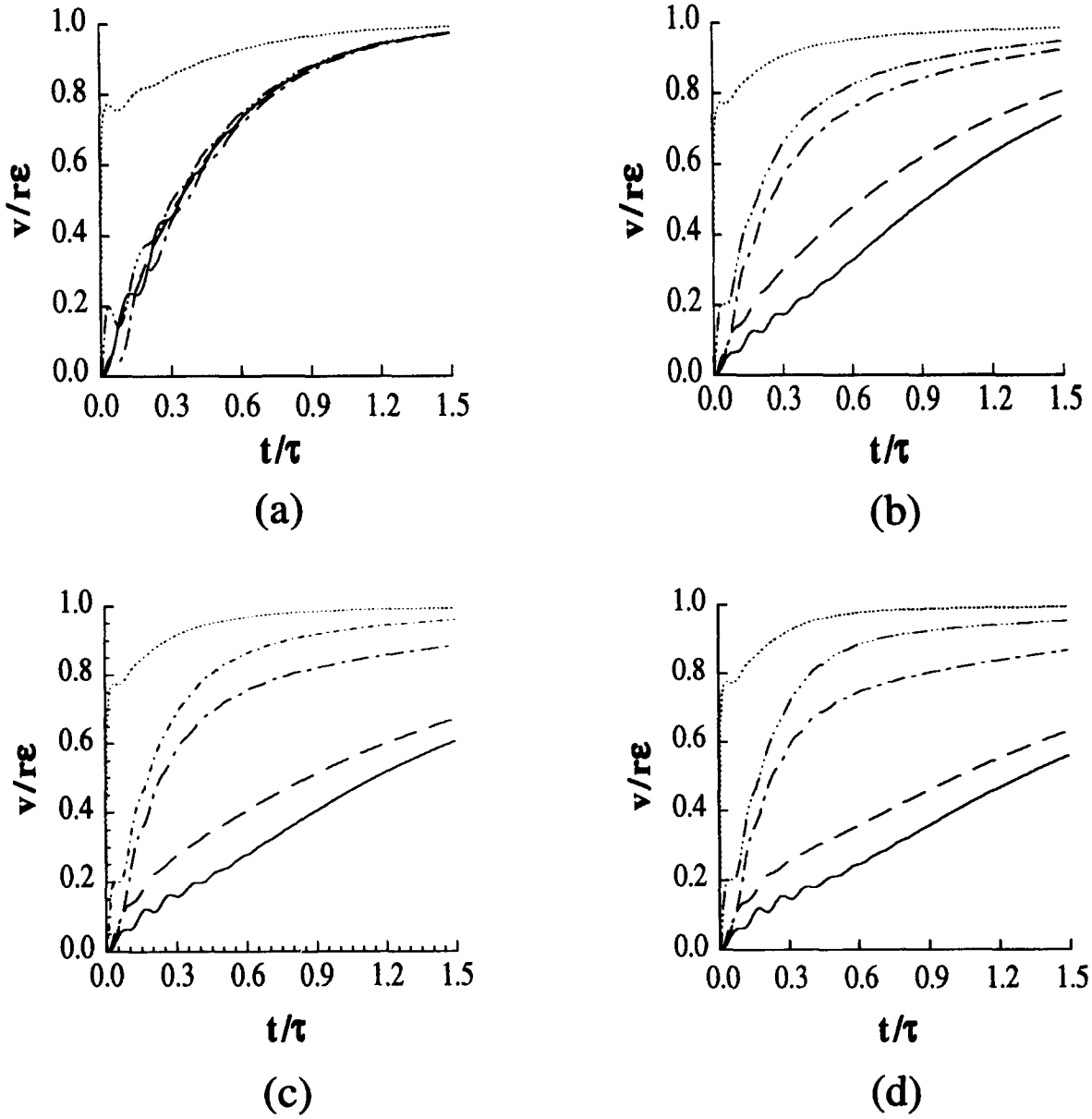

Figure 3 Same as in Figure 2, but at midradius $r=0.5$; axial positions z are $z=0.00$, ——; -0.21, – –; -0.40, —·—; -0.45, —···—; -0.49, ·····

ture, originating from the bottom endwall region, move to the large-radii region. At small and moderate radii, fluids of high temperature, originating from the midheight region, move downward by the counterclockwise meridional circulation. The magnitudes of perturbation temperature are substantial for the case of a single-diffusive fluid (Figure 8a). For a double-diffusive fluid, the global patterns of perturbation temperature field remain qualitatively unchanged. However, as is apparent in Figures 8b and c, the perturbation temperatures are very small in magnitude as R_ρ increases (note the difference in scales for the contour values of $\Delta T'$ in Figure 8). It is important to recognize that for a substantially stratified fluid, the temperature field in the course of spin-up is only slightly altered from the initial state linear profile when R_ρ is large. As can be inferred from Figures 7 and 8, for a double-diffusive fluid with large R_ρ, the perturbation density is contributed predominantly by the perturbation concentration, which is illustrated in Figure 9. For a strongly stratified fluid, as R_ρ increases, the magnitudes of S' increase and the iso-S' lines tend to cluster near the endwall.

Finally, the specific effect of the Lewis number Le is examined. Figure 10 shows that the rate of spin-up is generally retarded as Le increases. Combining the above computational results for the evolution of azimuthal velocity, a table has been made to show the nondimensional time to reach some arbitrarily defined value approaching the final state. In Table 1, these are tabulated for an exemplary interior location (near the midradius, quarter-height point) to reach $v/r\varepsilon = 0.7$. The weakening of the associated meridional circulation, as Le increases, is discernible in Figure 11. As can be seen in Figure 12, the perturbation density increases in magnitude as Le increases. This is at-

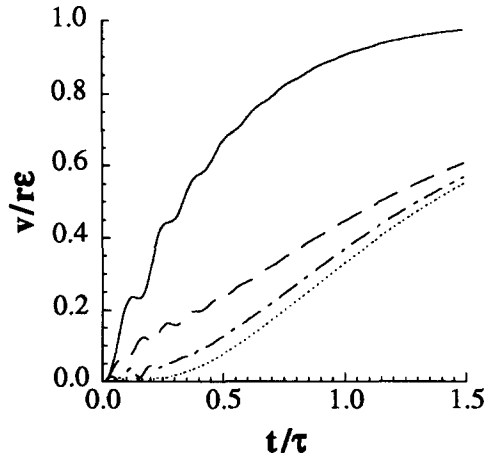

Figure 4 The effect of St on $v/r\varepsilon$ at midradius, midheight ($r=0.5$, $z=0$); $R_\rho=1.0$; St=0, ——; St=10, – –; St=30, —·—; St=100, ·····

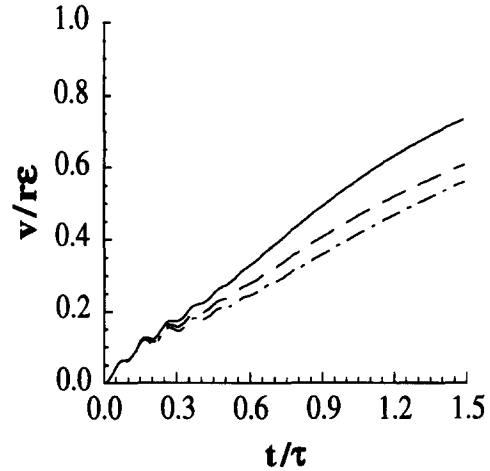

Figure 5 The effect of R_ρ on $v/r\varepsilon$ at midradius, midheight ($r=0.5$, $z=0$); St=10.0; $R_\rho=0$, ——; $R_\rho=1$, – –; $R_\rho=10$, —·—

tributable to the increase in perturbation concentration for large Le, as exhibited in Figure 13. When Le is large, thermal diffusion proceeds much faster than concentration diffusion. Therefore, the corresponding changes in perturbation temperature for large Le are meager.

In summary, for a double-diffusive fluid of a given St, the case of large Le is equivalent to an increase in the effective overall fluid stratification, which leads to a slowdown in the spin-up process. No published accounts have been reported on experimental measurements/observations of spin-up flows of a double-diffusive fluid. The numerical results of the present endeavor should be subject to experimental verifications.

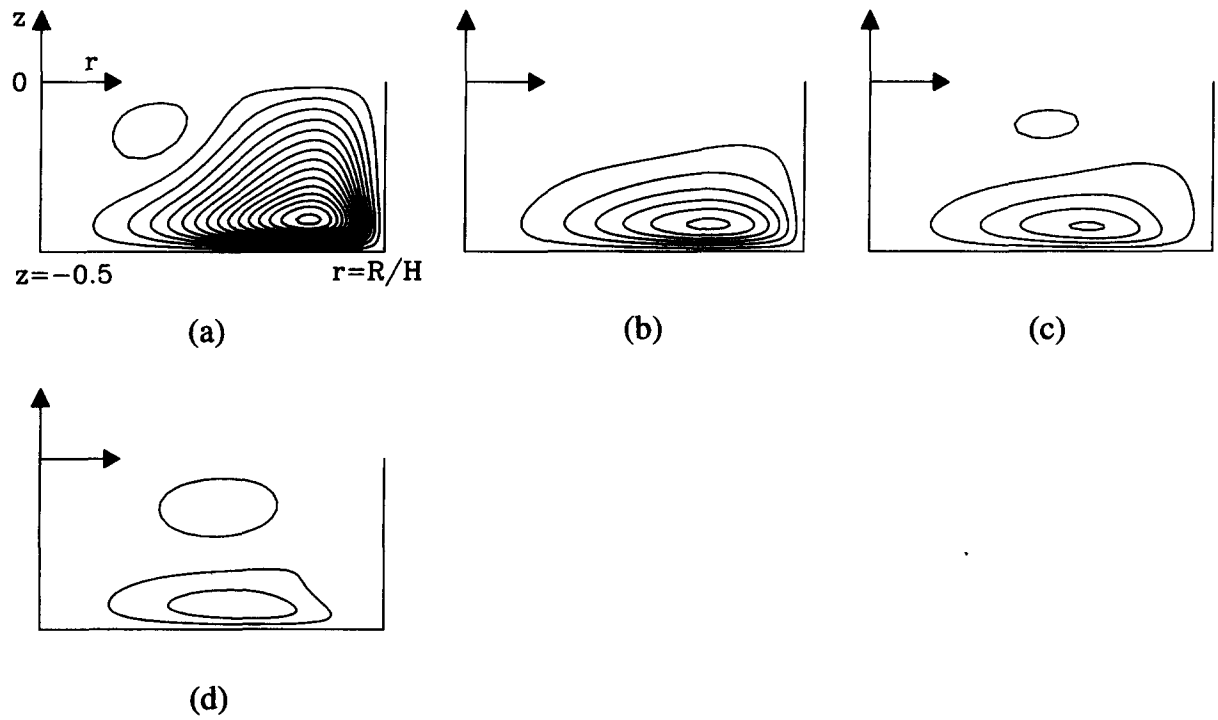

Figure 6 Plot of meridional stream function Ψ in the bottom half of the cylinder; conditions are Le=100.0, $t/\tau=0.282$; the contour increment is $\Delta\Psi=1.5\times10^{-4}$; (a) homogeneous fluid (St=0), $\Psi_{max}=2.25\times10^{-4}$; (b) single-diffusive fluid (St=10.0, $R_\rho=0$), $\Psi_{max}=8.70\times10^{-5}$; (c) double-diffusive fluid (St=10.0, $R_\rho=1$), $\Psi_{max}=5.47\times10^{-5}$; (d) double-diffusive fluid (St=10.0, $R_\rho=10$), $\Psi_{max}=3.62\times10^{-5}$

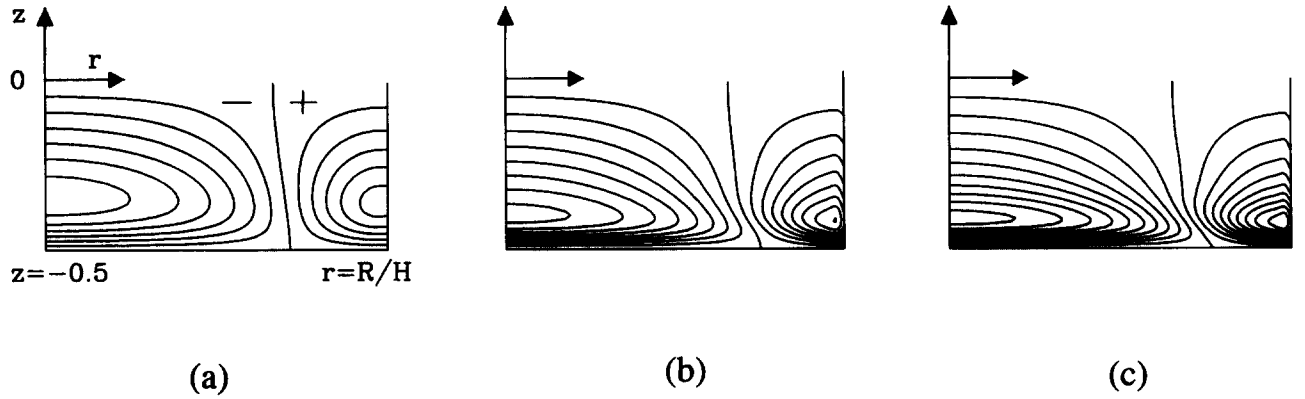

Figure 7 Plot of perturbation density ρ' in the bottom half of the cylinder; conditions St=10.0, Le=100.0, $t/\tau=0.282$; contour increment $\Delta\rho'=0.12$; (a) single-diffusive fluid ($R_\rho=0$), $\rho'_{max}=0.650$, $\rho'_{min}=0.794$; (b) double-diffusive fluid ($R_\rho=1.0$), $\rho'_{max}=0.963$, $\rho'_{min}=-1.01$; (c) double-diffusive fluid ($R_\rho=10.0$), $\rho'_{max}=1.18$, $\rho'_{min}=-1.26$

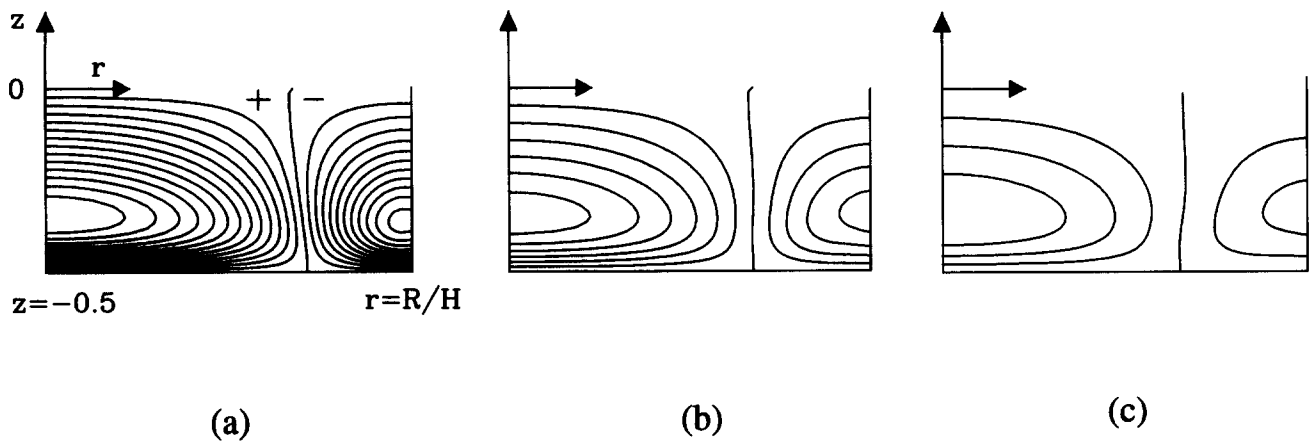

Figure 8 Plot of perturbation temperature T' in the bottom half of the cylinder; conditions St=10.0, Le=100.0, $t/\tau=0.282$; contour increment $\Delta T'=5.6\times10^{-2}$ for (a) and (b), and $\Delta T'=1.6\times10^{-2}$ for (c); (a) single-diffusive fluid ($R_\rho=0$); $T'_{max}=0.794$, $T'_{min}=-0.650$; (b) double-diffusive fluid ($R_\rho=1.0$); $T'_{max}=0.375$, $T'_{min}=-0.251$; (c) double-diffusive fluid ($R_\rho=10.0$); $T'_{max}=0.065$, $T'_{min}=-0.039$

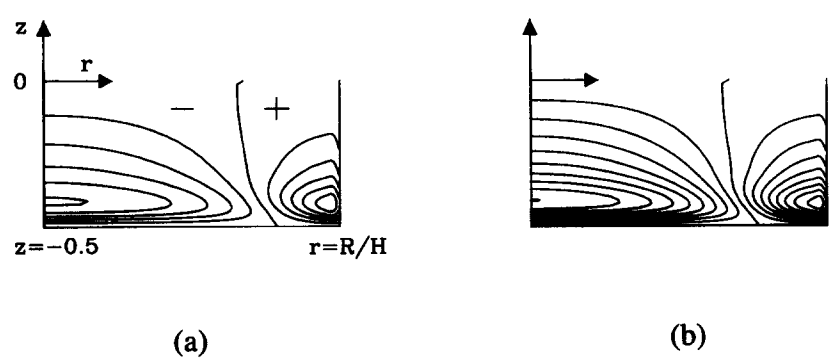

Figure 9 Plot of perturbation temperature S' in the bottom half of the cylinder; conditions St=10.0, Le=100.0, $t/\tau=0.282$; contour increment $\Delta S'=0.13$; (a) $R_\rho=1.0$, $S'_{max}=0.776$, $S'_{min}=-0.680$; (b) $R_\rho=10.0$, $S'_{max}=1.15$, $S'_{min}=-1.20$

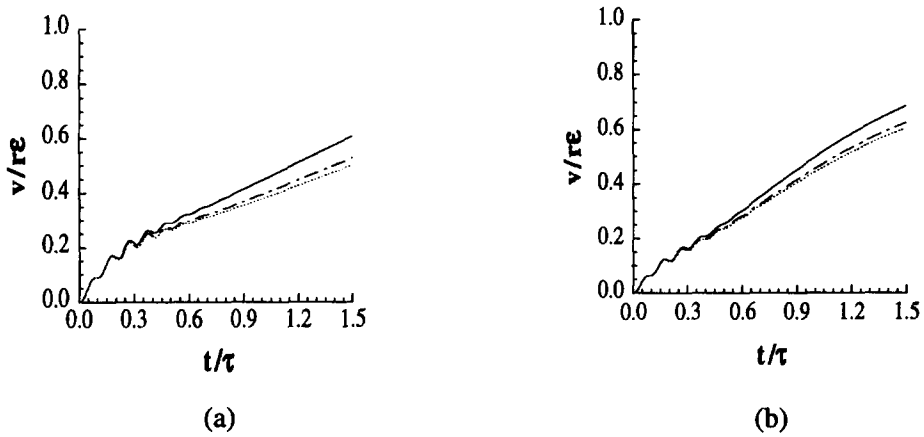

Figure 10 The effect of Le on $v/r\varepsilon$ at mid-depth $z=0$; conditions St=10.0, $R_\rho=1.0$ (a) $r=0.25$, (b) $r=0.50$; Le=2, ——; 10, —·—; 300, ·····

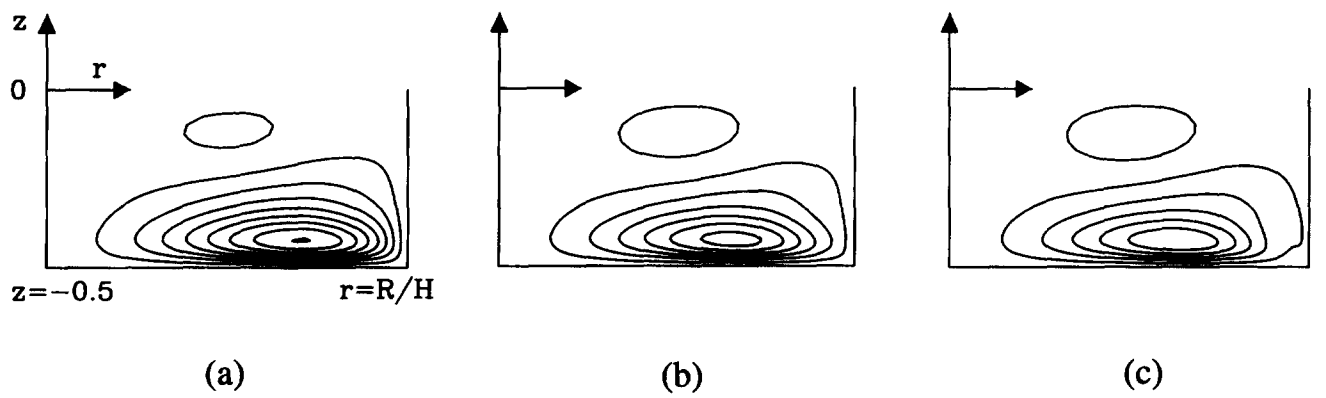

Figure 11 The effect of Le on Ψ, shown for the bottom half of the cylinder; conditions St=10.0, $R_\rho=1.0$, $t/\tau=0.282$; the contour increment $\Delta\Psi=6.6\times10^{-6}$; (a) Le=2.0, $\Psi_{max}=7.55\times10^{-5}$; (b) Le=10.0, $\Psi_{max}=5.97\times10^{-5}$; (c) Le=300.0, $\Psi_{max}=5.43\times10^{-5}$

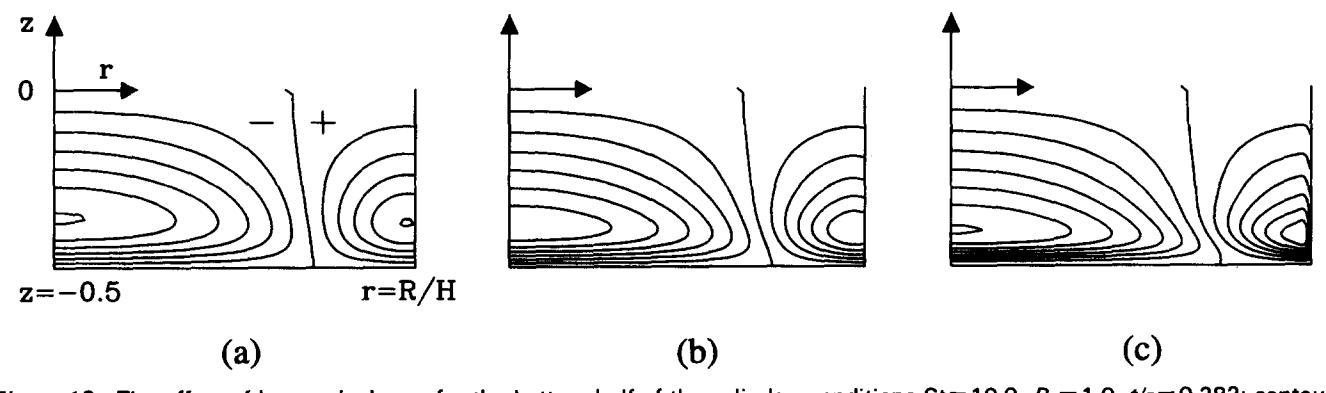

Figure 12 The effect of Le on ρ', shown for the bottom half of the cylinder; conditions St=10.0, $R_\rho=1.0$, $t/\tau=0.282$; contour increment $\Delta\rho'=0.14$; (a) Le=2.0, $\rho'_{max}=0.719$, $\rho'_{min}=-0.865$; (b) Le=10.0, $\rho'_{max}=0.854$, $\rho'_{min}=-0.967$; (c) Le=300.0, $\rho'_{max}=0.987$, $\rho'_{min}=-1.01$

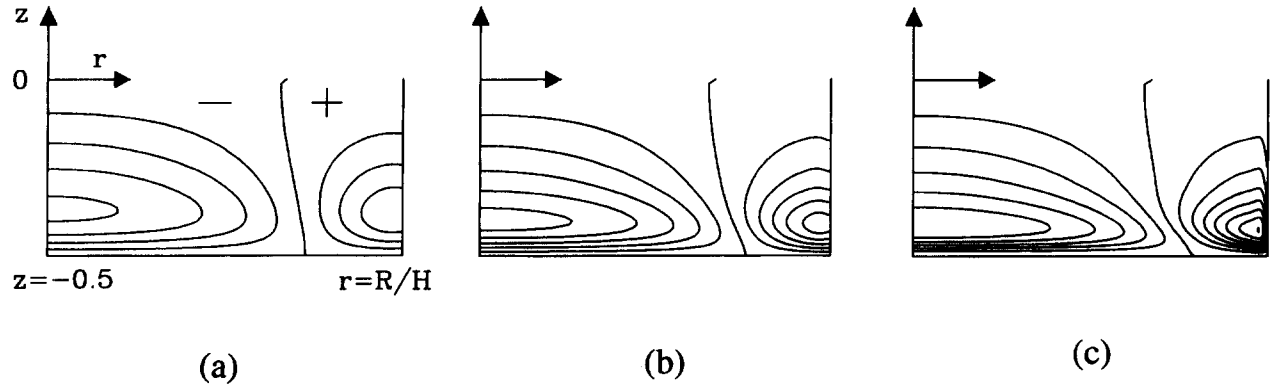

Figure 13 The effect of Le on S', shown for the bottom half of the cylinder; conditions St=10.0, R_ρ=1.0, t/τ=0.282; contour increment $\Delta S'$=0.11; (a) Le=2.0, S'_{max}=0.429, S'_{min}=−0.482; (b) Le=10.0, S'_{max}=0.631, S'_{min}=−0.619; (c) Le=300.0, S'_{max}=0.802, S'_{min}=−0.685

Table 1 Nondimensional times (t/τ) to reach $v/r\varepsilon$=0.7 at a location near the midradius, quarter-height point (r=0.5, z=−0.21)

Case	t/τ
Homogeneous	0.56
Single-diffusion (R_ρ=0)	1.12
R_ρ=1.0, Le=100	1.64
R_ρ=10.0, Le=100	1.80
Le=2.0, R_ρ=1.0	1.23
Le=10.0, R_ρ=1.0	1.48

Conclusions

For a double-diffusive fluid, the global spin-up process, as expressed by the evolution of the angular velocity field, is retarded. The attendant counterclockwise meridional circulation weakens in magnitude and shrinks in size toward the endwall. This retardation is more pronounced for large R_ρ. The rate of spin-up in the interior is spatially nonuniform for a stratified fluid. This spatial nonuniformity becomes notable for a double-diffusive fluid, as R_ρ increases.

The perturbation densities are negative(positive) in central(peripheral) areas of the meridional plane. The magnitudes of perturbation densities increase as R_ρ increases. For large R_ρ, the perturbation temperatures are very small in magnitude, but the magnitudes of perturbation concentration are appreciable.

Spin-up is retarded as Le increases. For large Le, the perturbation densities are caused mainly by the perturbation concentrations. As R_ρ increases and as Le increases, the situation is equivalent to increasing the general strength of effective global fluid stratification in the container.

Acknowledgment

The authors are grateful to the referees whose constructive comments led to improvements in the revised manuscript. This work was supported in part by a grant from the ministry of Science and Technology, Korea, under the International Cooperative Research Scheme, in collaboration with Prof. H. Ozoe of Kyushu University, Japan.

References

Brown, R. A. 1988. Theory of transport processes in single crystal growth from the melt. *AIChE J.*, **34,** 881–911

Buzyna, G. and Veronis, G. 1971. Spin-up of a stratified fluid: Theory and experiment. *J. Fluid Mech.*, **50,** 579–608

Greenspan, H. P. and Howard, L. N. 1963. On a time-dependent motion of a rotating fluid. *J. Fluid Mech.*, **17,** 385–404

Greenspan, H. P. 1980. A note on the spin-up from rest of a stratified fluid. *Geophys. Astrophys. Fluid Dyn.*, **15,** 1–5

Hayase, T., Humphrey, J. A. C. and Greif, R. 1992. A consistently formulated QUICK scheme for fast and stable convergence using finite-volume iterative calculation procedures. *J. Comp. Phys.*, **98,** 108–118

Hyun, J. M. 1983. Axisymmetric flows in spin-up from rest of a stratified fluid in a cylinder. *Geophys. Fluid Dyn.*, **23,** 127–141

Hyun, J. M., Fowlis, W. W. and Warn-Varnas, A. 1982. Numerical solutions for the spin-up of a stratified fluid. *J. Fluid Mech.*, 117, 71

Hyun, J. M. and Kwak, H. S. 1989. Flow of a double-diffusive stratified fluid in a differentially rotating cylinder. *Geophys. Astrophys. Fluid Dyn.*, **46,** 203–219

Hyun, J. M. and Lee, J. W. 1990. Double-diffusive convection in a rectangle with cooperating horizontal gradients of temperature and concentration. *Int. J. Heat Mass Transfer*, **33,** 1605–1617

Kobayashi, N. 1980. Computer simulation of heat, mass, and fluid flows in melt during Czochralski crystal growth. *Comp. Meth. Appl. Mech. Eng.*, **23,** 21–33

Lang, E., Sridhar, K. and Wilson, N. W. (1994). Computational study of disk driven rotating flow in a cylindrical enclosure. *J. Fluids Eng.*, **116,** 815–820

Lee, J. W. and Hyun, J. M. 1991a. Double-diffusive convection in a cavity under a vertical solutal gradient and a horizontal temperature gradient. *Int. J. Heat Mass Transfer*, **34,** 2423–2427

Lee, J. W. and Hyun, J. M. 1991b. Time-dependent double diffusion in a stably stratified fluid under lateral heating. *Int. J. Heat Mass Transfer*, **34,** 2409–2421

Ostarach, S., Jiang, D. and Kamotani, Y. 1987. Thermosolutal convection in shallow enclosures. *Proc. ASME-JSME Thermal Engr. Joint Conf.*, **2,** 159–168

Patankar, S. V. 1980. *Numerical Heat Transfer and Fluid Flow.* Hemisphere, Bristol, PA, 1090–1093

Sakurai, T. 1969. Spin-down problem of rotating stratified fluid in thermally insulated circular cylinders. *J. Fluid Mech.*, **36,** 689–699

Saunders, K. D. and Beardsley, R. C. 1975. An experimental study of the spin-up of a thermally stratified rotating fluid. *Geophys. Fluid Dyn.*, **7,** 1–27

Sung, H. J., Cho, W. K. and Hyun, J. M. 1993. Double-diffusive convection in a rotating annulus with horizontal temperature and vertical solutal gradients. *Int. J. Heat Mass Transfer*, **36,** 3773–3782

Sung, H. J., Jung, Y. J. and Ozoe, H. 1995. Prediction of transient oscillatory flow in czochralski convection. *Int. J. Heat Transfer*, **38,** 1627–1636

Turner, J. S. 1974. Double-diffusive phenomena. *Ann. Rev. Fluid Mech.*, **6,** 37–56

Walin, G. 1969. Some aspects of time-dependent motion of a stratified rotating fluid. *J. Fluid Mech.*, **36,** 289–307

Warn-Varnas, A., Fowlis, W. W., Piacsek, S. and Lee, S. M. 1978. Numerical solution and laser-Doppler measurements of spin-up. *J. Fluid Mech.*, **85,** 609–639

Wedemeyer, E. H. 1964. The unsteady flow within a spinning cylinder. *J. Fluid Mech.*, **20,** 383–399